475°C Embrittlement and Room Temperature Fatigue of Duplex Stainless Steel

Ken Wackermann[1], Jitendra Kumar Sahu[2] and Hans-Jürgen Christ[1]

[1]Universität Siegen, Institut für Werkstofftechnik
Paul-Bonatz-Strasse 9-11
57076 Siegen, Germany
[2]National Metallurgical Laboratory, Jamshedpur 831007, India

ABSTRACT

Duplex stainless steels (DSSs) are two-phase materials consisting of both the ferritic and the austenitic phase. The alloys are prone to embrittlement particularly in the temperature range between 280°C and 512°C. This so-called 475°C embrittlement is caused by a decomposition of the ferritic phase into a chromium-rich α' and an iron-rich α phase. The objective of this study is to develop a better understanding of the embrittling process of DSS of type SAF 2205. Embrittled and non-embrittled DSS was fatigue tested in stress-controlled tests at 475°C and in strain-controlled tests at room temperature. The high temperature fatigue tests were stopped at different cycle numbers in order to characterize the changing material conditions by means of room-temperature tensile tests and scanning electron microscopy pictures of the fracture surfaces.

KEYWORDS

Duplex Stainless Steel, 475°C Embrittlement, Fatigue Testing, Tensile Properties

INTRODUCTION

As dual-phase materials DSSs excellently combine reasonable mechanical properties and high chemical resistance [1,2]. Therefore, DSSs are mainly used in the offshore and chemical industry [3,4]. Unfortunately, DSS are very prone to different types of embrittlement, which deteriorate the material properties, such as tensile strength, fatigue behavior and impact strength significantly [5–9]. In particular the 475°C embrittlement limits the usage of the DSS to temperatures below the temperature of embrittlement.

MATERIALS, SPECIMENS AND TESTING

Materials

The duplex stainless steel (DSS) of type SAF 2205 used in this study was delivered as cast bars in two heats, Table 1.

Element	C	Si	Mn	P	S	Cr	Ni	Mo	N
Heat 1	0.020	0.53	1.83	0.02	0.002	22.0	5.6	3.1	0.19
Heat 2	0.056	0.33	1.59	<0.0005	<0.0005	22.6	5.5	2.8	0.45

Table 1: Chemical composition in mass % of the tested DSSs

A first standard heat treatment of 4 hours at 1250°C, followed by a linear cooling over 3 hours to 1050°C with final water quenching was used to prepare the specimens of the non-embrittled material condition. For the embrittled material condition a second heat treatment was applied consisting of 100 hours at 475°C with final air cooling.

Specimens and Testing

Fatigue tests were carried out in a MTS push-pull servohydraulic testing machine in laboratory air on specimens with a cylindrical gauge length of 18 mm in length and 5 mm in diameter. The surface of the gauge length was firstly mechanically polished and finally electrolytically polished at -25°C with 10 V with an electrolyte consisting of 700 ml ethanol, 120 ml distilled water, 100 ml diethyleneglycolmono-n-buthylether and 80 ml of 60% perchloric acid. Specimens of heat 1 were fatigued at room temperature in strain-control at total strain amplitudes of $\Delta\varepsilon/2 = 4x10^{-3}$, $6x10^{-3}$, $8x10^{-3}$ and $1x10^{-2}$ at 0.5 Hz. The tests of specimens of heat 2 were performed at 475°C through induction heating in stress control at a stress amplitude of 375 MPa and a stress ratio of R = -1 with a sinusoidal wave-form and a frequency of 2 Hz. At 100, 1000 and 20,000 cycles the fatigue tests of heat 2 were interrupted and the specimens air-cooled for tensile testing at room temperature. Furthermore, samples of heat 2 were solely aged for 50, 500 and 10,000 s which corresponds to the testing times in the fatigue experiments.

RESULTS AND DISCUSSION

Effects of embrittlement on charpy impact and ultimate tensile behaviour

The difference between the initial ultimate tensile strength (UTS) for non-embrittled DSS and the maximum UTS for embrittled DSS is about 250 MPa, Table 2. About 40% of this difference is already obtained after 10,000 s at the embrittlement temperature, whereas the final 60% take nearly 100 h. In other words the UTS increases rapidly in the beginning and then slows down to a lower rate of increase. The change of the material properties is even more visible in the charpy impact strength (CIS). After 10,000 s a very drastic drop of nearly 80% is observed, Fig. 1. The final and minimum CIS is reached after 100 h with a drop of 90% from the starting value. A fast change of the material properties such as UTS, CIS and hardness in the beginning is a typical material behaviour of DSSs [10,5]. Pohl and Ibach [10] explain the slower increase of the tensile strength of DSS for advanced aging times with the crack initiation model of Cottrell. This assumes a microcrack initiation in the ferritic phase hindering an ongoing fast increase of the UTS caused by the embrittlement [10]. As conclusion, the CIS and the UTS are both very good indicators for the embrittlement. Furthermore, the DSS is fully embrittled after 100 h because the impact tests do not show a further reduction of CIS for longer aging times.

Aging Time	0 s	50 s	500 s	10,000 s	Fully-Embrittled
Ultimate Tensile Strength	795 MPa	798 MPa	871 MPa	891 MPa	1045 MPa
Reduction of Area	61 %	61 %	62 %	63 %	39 %

Table 2: Effect of the 475°C aging on the ultimate tensile strength and the reduction of area for various aging times of heat 2

In contrast the fracture surfaces appearances and the reduction of area (ROA) after fracture are less suitable indicators for the embrittlement than the UTS and the CIS. For all aging

times (0 s, 50 s, 500 s, 10,000 s) the fracture surfaces of heat 2 show a ductile fracture surface with dimples and a constant ROA of about 61%, Fig. 2 and Table 2. Solely the fully-embrittled specimens show a brittle fracture surface with planar areas and a strong reduced ROA of 39%. The slower change of the fracture morphology from ductile to brittle fracture mode is consistent with the results reported by other researches. Pohl and Ibach [10] recognised a change from ductile to brittle fracture surfaces firstly after 5 hours at maximum embrittlement temperature. Hilders et al. [11] found a first brittle appearance after 6.5 hours and an obvious brittle fracture surface only after 24 hours. As a consequence the aging time of 10,000 s is too short for a sufficient change of the microstructure towards a brittle fracture behaviour. As a result the application of the DSS is usually limited to the temperature of embrittlement, because even short aging times result in an unfavourable change of UTS and CIS.

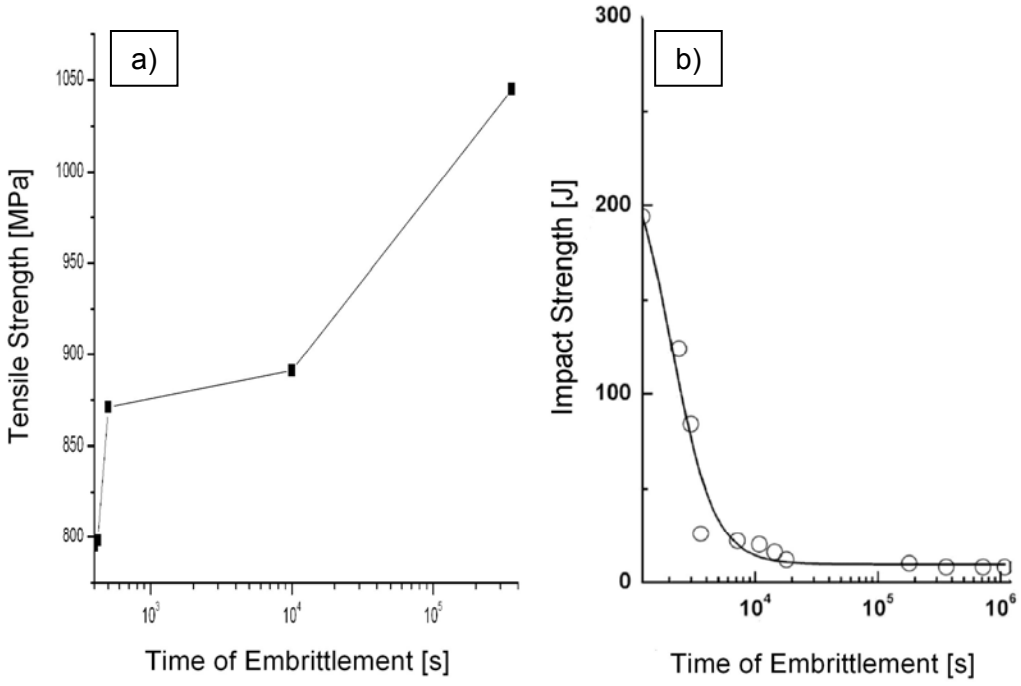

Fig. 1: Effect of 475°C aging on (a) the ultimate tensile strength of DSS of heat 2 and (b) on the charpy impact strength of heat 1

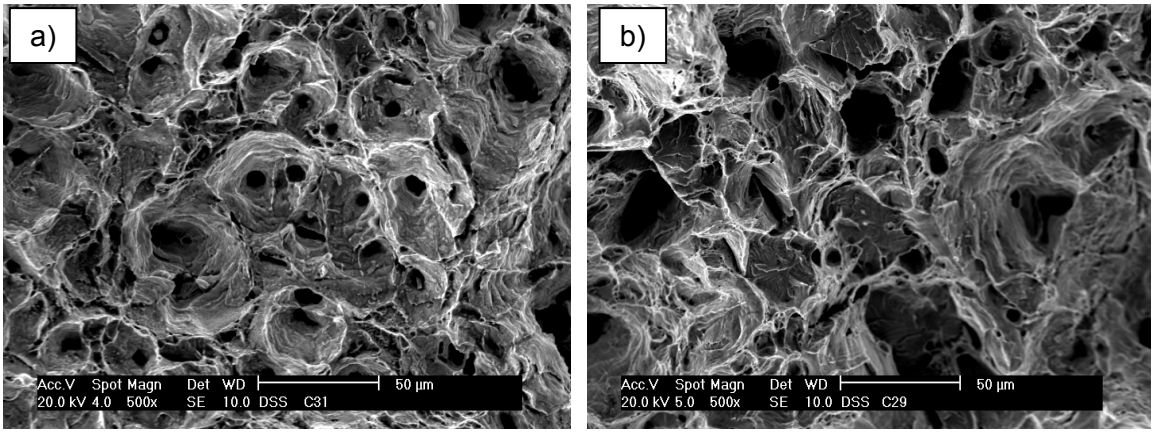

Fig. 2: Tensile test fracture surfaces of (a) non-embrittled and (b) embrittled DSS of Heat 2

Effect of embrittlement on room temperature fatigue

The cyclic deformation curves of room temperature fatigue tests are illustrated in Fig. 3 in the representation of the stress amplitude Δσ/2 vs. the cyclic number N.

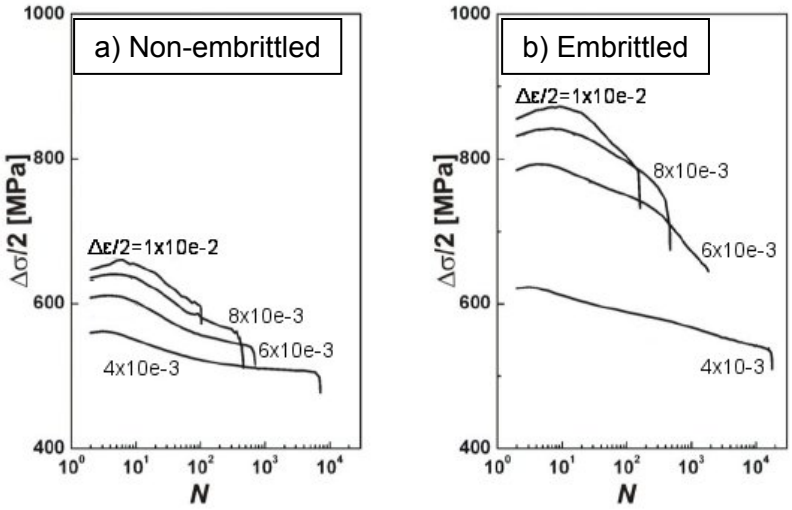

Fig. 3: Cyclic deformation curves of room temperature fatigue tests of (a) non-embrittled and (b) embrittled condition in total strain control of $\Delta\varepsilon/2 = 4x10^{-3}$, $6x10^{-3}$, $8x10^{-3}$ and $1x10^{-2}$

For both material conditions a higher strain amplitude leads to higher stress response and shorter number of cycles to failure. Embrittled DSS has a higher stress response and a more pronounced cyclic softening as non-embrittled DSS. For all fatigue tests a short period of cyclic hardening in the beginning is followed by extensive cyclic softening. One reason for the difference in the cyclic behavior of embrittled and non-embrittled DSS is given by Armas et al. [9] who suggest a microstructure change in the ferritic phase. Llanes et al. [12] explicitly state a partial demodulation of the spinodal decomposition of the ferritic phase. The room temperature Coffin-Manson plot documents in Fig. 4 that cyclic life is primarily determined by the plastic strain amplitude and that the behaviour of both conditions in terms of $\Delta\varepsilon_{pl}/2$ is very similar.

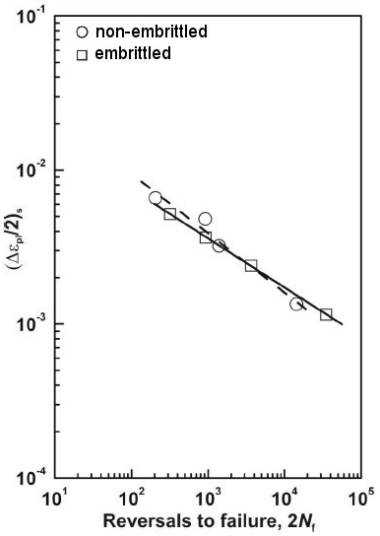

Fig. 4: Room temperature Coffin-Manson plot comparing the life data of the embrittled and the non-embrittled condition

However, there is a tendency that that non-embrittled DSS has a better fatigue resistance than embrittled DSS for high plastic strain amplitudes and vice versa .A similar behaviour was observed by Vogt et al. [13]. The fracture surfaces of the tensile tested specimens show ductile fracture surfaces with dimples for non-embrittled DSS, whereas in the embrittled DSS also cleavage cracks were detected.

475°C fatigue behaviour of embrittled and non-embrittled DSS

Embrittled and non-embrittled samples of heat 2 were fatigued at 475°C with 2 Hz applying a stress amplitude of 375 MPa. For 100, 1000 and 20,000 cycles the fatigue tests were stopped for room temperature tensile tests. The cyclic deformation curves of two fatigue tests performed until failure are shown in Fig. 5 in the representation of the plastic strain amplitude versus the cycle number and show distinct differences in the material behaviour for the two conditions. Non-embrittled DSS exhibits a pronounced cyclic hardening in the first 20 cycles in comparison to very low cyclic hardening for embrittled DSS. After 20 cycles the plastic strain amplitudes of both material conditions are very similar and remain almost identical in a slow monotonic decrease until failure. Since the testing time of 20 cycles is too short for embrittlement, as the CIS and UTS show, the cyclic hardening in high-temperature stress-controlled tests does not seem to depend primarily on the embrittlement process but rather on the cyclic deformation. This is supported by the observation, that the plastic strain amplitude remains almost identical for the rest of the test, because a further decrease of the cyclic deformation curves for the non-embrittled specimens due to the ongoing embrittlement would be expected. That holds true only for stress-controlled high-temperature fatigue testing as can be seen from the results of Armas et al. [9] for strain-controlled high-temperature fatigue tests of DSS.
Some non-embrittled specimens were found to reach the limit number of load cycles of 2×10^5, whereas embrittled specimens fractured at lower cycle numbers. This is supported by a slower crack propagation of the non-embrittled DSS in comparison to the embrittled DSS in constant ΔK crack propagations tests [14–16].
Table 3 shows the values of UTS and ROA from tensile tests after discontinued fatigue tests at 475°C and compares the effect of fatigue loading on embrittled and non-embrittled DSS. The aging times of solely aged specimens listed in Table 2 correspond to the testing times of the fatigue tests. The UTS at fracture of the non-embrittled and solely aged samples is very similar to the ones of the non-embrittled and 475°C fatigued specimens. Furthermore the UTS of the embrittled DSS is constant for all tests irrespective of the number of load cycles at 475°C. Therefore, it can be concluded that the tensile strength depends only on the prior aging treatment and not on the subsequently applied fatigue load of $\Delta\sigma/2$ = 375 MPa. Interestingly, the ROA of the non-embrittled and solely aged DSS or the non-embrittled and fatigued DSS is the same for all tests. The results above indicate that the testing time of 20,000 cycles is too short for a strong embrittlement. Furthermore the embrittlement process seems to be only time dependent and is not affected by a superimposed mechanical load cycle. This conclusion is supported by the fracture surfaces for non-embrittled fatigued or solely aged DSS as the fracture surfaces are very similar and do not show brittle areas, Fig. 6 and Fig. 2. Again the time at embrittlement temperature is too short for a change in the fracture morphology.
Interestingly, the ROA for embrittled DSS is almost constant for the fatigue (1000 cycles, 36%, Table 3) and non-fatigued (39%, Table 2) conditions. However, at 20,000 cycles the ROA has reduced to 16%. This decrease may be a consequence of a secondary hardening, which takes place at some 20,000 cycles, Fig. 5. As the micrograph in Fig. 6b suggests, this hardening may be a result of a microstructure change. The fracture surface reveals many planar fracture areas which are not present in the non-fatigued embrittled DSS, Fig. 2b.

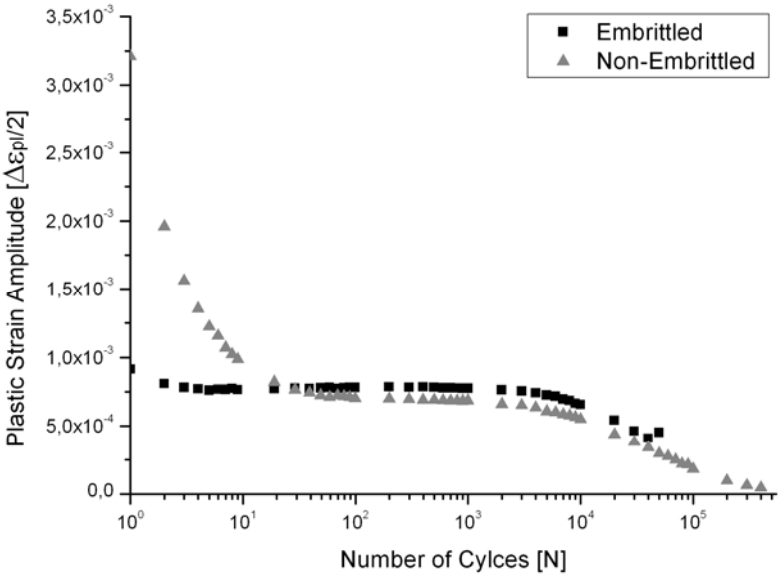

Fig. 5: Cyclic plastic deformation curves until failure for embrittled and non-embrittled DSS fatigued at 475°C at a stress amplitude of 375 MPa and 2 Hz

Material Condition	Number of loading cycles		
	100 cycles	1000 cycles	20,000 cycles
Non-Embrittled (UTS / ROA)	840 MPa / 59%	846 MPa / 61 %	905 MPa / 61 %
Embrittled (UTS / ROA)	- / -	1047 MPa / 36 %	1057 MPa / 16 %

Table 3: Effects of 475°C fatigue on ultimate tensile strength and reduction of area

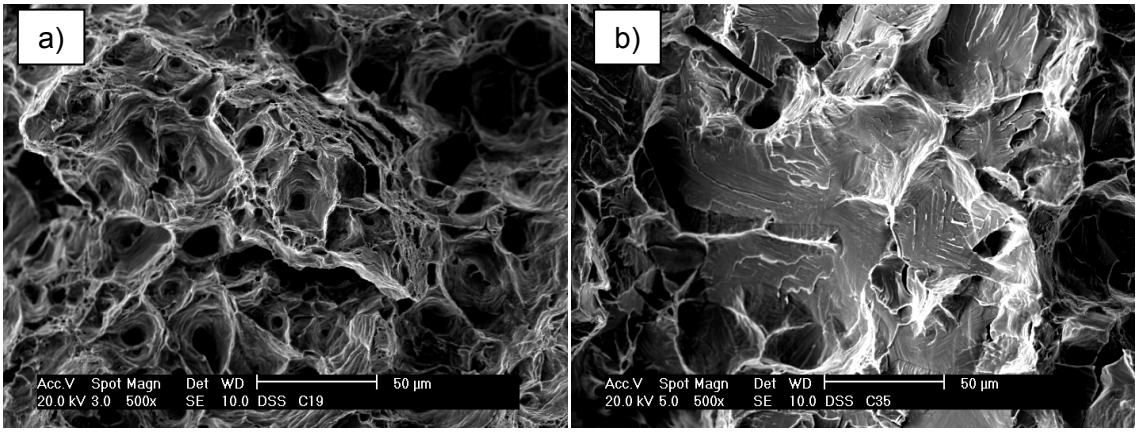

Fig. 6: Fracture surfaces of (a) non-embrittled and (b) embrittled specimens having seen 20,000 fatigue cycles

SUMMARY AND CONCLUSION

Embrittled and non-embrittled samples of duplex stainless steel were fatigue tested at a stress amplitude of 375 MPa at 475°C. The fatigue tests were discontinued after 0, 100, 1000 and 20,000 cycles for tensile testing. A second heat of this material was room temperature fatigued in strain control. For comparison non-embrittled specimens were aged for the corresponding times of 0, 100, 1000 and 20,000 cycles before tensile testing. The

fracture surfaces and the cyclic stress-strain behaviour and the fatigue lives were compared leading to the following conclusion:

- The ultimate tensile strength and the charpy impact strength UTS do not depend on the cycle load but only on the aging time at 475°C. The increase in strength is fastest in the first hours of testing and reaches a constant value after long time.
- Only non-embrittled DSS shows pronounced cyclic hardening in stress-controlled fatigue tests of 475°C in the first 20 cycles. The main reason for this hardening is the high resulting plastic strain amplitude of non-embrittled DSS. The cyclic hardening mainly results from the cyclic plastic deformation and not from the embrittlement. However the cyclic curves for embrittled and non-embrittled DSS coincide.
- The evaluation of the strain-controlled fatigue tests has revealed that the Coffin-Manson plot shows better fatigue resistance for embrittled DSS in the low plastic strain regime. For high plastic strain the non-embrittled condition exhibits longer fatigue life.
- The tensile fracture surfaces show prevailing ductile fracture for all specimens expect the fully embrittled specimen. Therefore the maximum testing length of 20,000 cycles, which corresponds to 10,000 s is too short to significantly change these material properties towards embrittlement condition.
- The reduction of area is smaller for embrittled DSS than for non-embrittled DSS.

ACKNOWLEDGMENT

The Deutsche Forschungsgemeinschaft (DFG) is gratefully acknowledged for financial support of this study.

REFERENCES

[1] Alvarez-Armas, I.; Marinelli, M.; Hereñú, S.; Degallaix, S., Armas, A.:
On the cyclic softening behaviour of SAF 2507 duplex stainless steel
Acta Materialia 54 (2006) No. 19, pp. 5041–5049

[2] Calliari, I.; Brunelli, K.; Zanellato, M.; Ramous, E., Bertelli, R.:
Microstructural modification during isothermal ageing of a low nickel duplex stainless steel
Journal of Materials Science 44 (2009) No. 14, pp. 3764–3769

[3] Akdut, N.:
Phase morphology and fatigue lives of nitrogen alloyed duplex stainless steels
International Journal of Fatigue 21 (1999) No. 1 Supplement 1, pp. 97–103

[4] Iacoviello, F.; Boniardi, M., La Vecchia, G.:
Fatigue crack propagation in austeno-ferritic duplex stainless steel 22 Cr 5 Ni
International Journal of Fatigue 21 (1999) No. 9, pp. 957–963

[5] Weng, K.; Chen, T., Yang, J.:
The high-temperature and low-temperature aging embrittlement in a 2205 duplex stainless steel
Bulletin of the College of Engineering 89 (2003), pp. 45–61

[6] Grobner, P.:
The 885°F (475°C) embrittlement of ferritic stainless steels
Metallurgical Transactions 4 (1973) No. 1, pp. 251–260

[7] Zieliński, W.; Świątnicki, W.; Bartsch, M., Messerschmidt, U.:
Non-uniform distribution of plastic strain in duplex steel during TEM in situ deformation
Materials Chemistry and Physics 81 (2003) No. 2-3, pp. 476–479

[8] Hereñú, S.; Alvarez-Armas, I., Armas, A.:
Microstructural changes in a duplex stainless steel during low cycle fatigue
Materialprüfung / Bundesanstalt für Materialforschung und -prüfung 51 (2009) No. 6, pp. 359–364

[9] Armas, A.; Herenu, S.; Degallaix, S., Condó, A.:
Temperature influence on the cyclic behaviour of aged and unaged super duplex stainless steels
in: Duplex Stainless Steel World Conference (2007) No. 16.pdf, pp. 1–12

[10] Pohl, M., Ibach, A.:
Gefüge und Gebraucheigenschaften für Super-Duplexstähle
Praktische Metallographie 28 (1991) No. 7, pp. 333–349

[11] Hilders, O.; Sáenz, L.; Ramos, M., Peňa, N.:
Effect of 475°C embrittlement on fractual behaviour and tensile properties of a duplex stainless steel
Journal of materials engineering and performance: design, process, characterization, evaluation / A 8 (1999) No. 1, pp. 87–90

[12] Llanes, L.; Mateo, A.; Iturgoyen, L., M. Anglada, M.:
Aging effects on the cyclic deformation mechanisms of a duplex stainless steel
Acta Materialia 44 (1996) No. 10, pp. 3967–3978

[13] Vogt, J.-B.; Massol, K., Foct, J.:
Role of the microstructure on fatigue properties of 475°C aged duplex stainless steels
International Journal of Fatigue 24 (2002) No. 6, pp. 627–633

[14] Calonne, V.; Gourgues, A., Pineau, A.:
Fatigue crack propagation in cast duplex stainless steels: thermal ageing and microstructural effects
Fatigue Fract Engng Mater Struct 27 (2004) No. 1, pp. 31–43

[15] Casari, F.; Di Cocco, V.; Iacoviello, F., Ischa, G.:
Chemical composition influence on duplex stainless steels 475°C embrittlement
in: Duplex Stainles Steels World Conference, 2007 No. 36.pdf, pp. 1–9

[16] Iturgoyen, L.; Mateo, A.; Llanes, L., Anglada, M.:
Mechanical behaviour of duplex stainless steels aged at low temperatures (275-475°C)
in: Stainless Steels '96, Stahleisen, Düsseldorf, 1996, pp. 355–356

Corresponding author: wackermann@ifwt.mb.uni-siegen.de